Atmospheric Environment Vol. 9, pp. 145–174. Pergamon Press 1975. Printed in Great Britain.

SIMULATION OF THE PLANETARY BOUNDARY LAYER IN A MULTIPLE-JET WIND TUNNEL*

H. W. TEUNISSEN†

Institute for Aerospace Studies, University of Toronto, 4925 Dufferin Street, Downsview, Ontario, Canada M3H 5T4

(*First received* 6 *August* 1973 *and in final form* 7 *February* 1974)

Abstract—A new method has been devised for generating turbulent shear flows with nearly independently controlled mean velocity and turbulence intensity characteristics and in particular, for simulating neutrally stable planetary boundary layer flows. The method involves the use of a small, open-circuit wind tunnel which is driven on the ejector principle by an array of 64 jets whose velocities may be individually controlled. By appropriate adjustment of these velocities, two-dimensional turbulent flows possessing virtually any desired mean velocity profile at any plane in the test section of the tunnel have been produced. With the use of simple "tripping" barriers and varying degrees of surface roughness, differing turbulence levels have been obtained for flows with virtually identical mean velocity profiles. Reasonable simulations of the flow in the planetary boundary layer over differing types of terrain have been achieved with respect to both mean velocity and turbulence characteristics.

NOMENCLATURE

A_j	total cross-sectional area of jets in grid, ft^2
A_s	total open cross-sectional area in jet exit plane, ft^2
H	tunnel height = 8 in.
k	reduced frequency n/U, cycles ft^{-1}
L_u, L_v, L_w	integral scale of u, v, w components, respectively, ft
M	mesh length of jet grid = 1 in.
n	frequency, Hz
u	longitudinal turbulent velocity component, ft s^{-1}
u'	$\sqrt{u^2}$, ft s^{-1}
U	mean (time-averaged) longitudinal velocity component, ft s^{-1}
U_c	mean velocity on tunnel centreline, ft s^{-1}
U_j	jet exit velocity, ft s^{-1}
U_{j0}	reference value of jet exit velocity = 180 ft s^{-1} unless otherwise specified
U_0	reference flow velocity, ft s^{-1}
U_δ	gradient velocity, ft s^{-1}
U_τ	friction velocity, ft s^{-1}
v	lateral turbulent velocity component, ft s^{-1}
v'	$\sqrt{v^2}$, ft s^{-1}
w	vertical turbulent velocity component, ft s^{-1}
w'	$\sqrt{w^2}$, ft s^{-1}
x	longitudinal coordinate
y	lateral coordinate
z	vertical coordinate
z_0	roughness length, ft
α	power-law velocity profile index
$\Gamma_u(k, z_1, z_2)$	narrow-band cross-correlation function = $\phi_u(k, z_1, z_2)/[\phi_u(k, z_1)\phi_u(k, z_2)]^{1/2}$
δ	gradient height or boundary layer thickness, ft
$\phi_u(k)$, $\phi_v(k)$, $\phi_w(k)$	power spectral densities of u, v and w components, respectively, ft^3 cycle^{-1} s^{-2}
$\phi_u(k, z_1, z_2)$	longitudinal component cross-spectrum between points z_1 and z_2, ft^3 cycle^{-1} s^{-2}
$\phi_u(k, z_1)$, $\phi_u(k, z_2)$	longitudinal component power spectra at points z_1 and z_2, respectively, ft^3 cycle^{-1} s^{-2}.

* Presented at the 4th Canadian Congress of Applied Mechanics held at Montreal, Canada, 28 May to 1 June, 1973.

† Present affiliation: Atmospheric Environment Service, 4905 Dufferin Street, Downsview, Ontario, Canada M3H 5T4.

1. INTRODUCTION

In recent years, there has been an increasing interest in the effect of flows in the atmospheric, or planetary, boundary layer on various structures and flow processes in it. This has been brought about by the appearance of important problems in several areas. In the aerospace field, for example, problems such as the response of slow low-flying VTOL and STOL aircraft to these flows are of major importance, as is the effect of ground wind loads on tall launch vehicles. In the realm of architectural or industrial aerodynamics, the behaviour of buildings and structures subjected to atmospheric flows is becoming increasingly important, particularly in view of the apparently unlimited complexity being designed into them by present-day architects. Not only is the aeroelastic response of these structures themselves important, but also the environmental effects of the wind flows around them are of significant interest. In addition, the dispersion of particulate matter and diffusion processes in the atmosphere are presently of prime concern as a result of the increasing awareness of pollution as a problem. It can be seen, therefore, that the effect of the flow in the planetary layer is of major importance in many varied disciplines.

Because of the extreme complexity of the flows in the planetary layer, analytical approaches to the solution of many of the problems described above become extremely difficult, and rather drastic simplifications are usually required. This is particularly so in cases where the effects of the wind at any point are strongly dependent on the turbulent wakes and vortex shedding phenomena created by surrounding structures. For reasons such as these, many problems are best attacked experimentally under controlled conditions, and consequently the capability of simulating planetary flows in laboratory wind tunnels has become increasingly important.

There are at present two basic methods in use for simulation of the planetary boundary layer in a wind tunnel. The first of these involves the use of a boundary layer wind tunnel, in which a long, rough surface is used to grow a "natural" boundary layer. The roughness of the surface serves to accelerate the growth of the layer to a workable thickness, but a very long test section is still required, and this is the main drawback of this approach. Boundary layer tunnels are presently used by many investigators (e.g. Cermak, 1970; Davenport and Isyumov, 1968) and form the basis of most of the experimental work presently being performed. The second method involves the use of various devices to create an artificially thick boundary layer flow, followed by a rough surface which will maintain the turbulence levels created by the device. The principle advantage of this method lies of course in the absence of a long fetch length necessary to create a reasonably thick flow. A variety of devices have been used in this approach, with varying degrees of success. Grids of rods or slats employing varying spacing between the rods are often used (Vickery, 1965) while curved screens have been used to obtain desired velocity profiles (Baines, 1963; Lau, 1966). Horizontal roughness plates with varying spacing have also been investigated (Strom and Kaplan, 1960). At the National Research Council of Canada, combinations of grids and "spires" have been used (Templin, 1969; Standen, 1972) while Counihan (1969, 1970) has successfully used so-called "elliptic wedge generators" and barriers to obtain reasonable flows. Ludwig and Sundaram (1969) have also used horizontal barrier plates of various heights across the tunnel floor, in conjunction with vortex generators in some cases, while Schon and Mery (1971) have studied the effects of a "barrier" created by a vertical, two-dimensional jet of air blowing from the floor of the test section.

While all the above methods of the second type have attained some degree of success in simulating the planetary layer, they nearly all suffer from a basic inflexibility arising

from the interdependence of the mean velocity and turbulence characteristics in the flows produced. That is, trial-and-error methods are used to create a desired velocity profile in the test section of the tunnel. However, the turbulence levels achieved may not be those desired and it is in general quite difficult to alter these characteristics without adversely affecting the velocity profile. Consequently a great deal of effort is often required to obtain a reasonable compromise for each particular flow.

Some time ago it was decided at UTIAS to investigate the capability of a wind tunnel utilizing a grid of jets blowing downstream for creating turbulent flows. The jets themselves could be used to drive the wind tunnel on the ejector principle, with turbulence resulting from the shear between the primary and secondary flows. Thus the entire grid of jets would act, in effect, like a "negative" grid of rods. Furthermore, if enough jets were used, turbulent shear flows possessing virtually any desired velocity profile might be created by variation of the flow velocity in each jet. A small model tunnel was constructed and an experimental investigation into the feasibility of this "ejector-driven" or "multiple-jet" wind tunnel was undertaken (Teunissen, 1969). The results of this investigation showed that the concept was indeed feasible in that uniform turbulent flows quite similar to those obtained behind conventional grids of rods could be produced, and the possibilities for the creation of shear flows appeared promising. Consequently some modifications to the tunnel were made and further investigation was undertaken. This work was concerned primarily with determining the suitability of the tunnel for producing turbulent shear flows with arbitrary characteristics and in particular, for producing simulations of the flows in the planetary boundary layer. The principle advantage of simulation with this tunnel would lie in an ability to control velocity profiles with the jets independently of any turbulence producing devices that might be necessary in the flow. Also, variation of the velocity profile would be quite simple with the use of the jets and thus the difficulty of achieving a desired combination of mean velocity and turbulence characteristics would be greatly reduced. In terms of the two basic simulation methods described above, then, the multiple-jet tunnel would represent an improved version of the second method, and ideally a very long test section would not be required in order to develop a desired flow.

The present paper outlines the experimental investigations referred to above and presents the results that have been obtained. In general, the flow properties considered in this work were the mean velocity through the flow, the intensities of the three turbulent velocity components, correlations of the components, power and cross-spectral densities, integral scales and Reynolds stresses. A description of the model wind tunnel and the instrumentation used to make these measurements is presented initially, followed by some basic characteristics of the tunnel which were obtained in a flow having a uniform mean velocity profile. Some general characteristics of planetary boundary layer flows are then outlined and the results of our attempts to simulate these flows are discussed in detail. Finally the results of attempts to generate various degrees of linear shear flow are described and a brief summary of the conclusions is presented. Further details of all the equipment and results described here can be found in Teunissen (1972).

2. EXPERIMENTAL APPARATUS AND INSTRUMENTATION

2.1 *Wind tunnel and associated equipment*

The model wind tunnel used in this experiment is an open-circuit tunnel which is driven by an array of 64 jets. Its cross-section is eight inches square and it consists of several interchangeable sections which can produce a maximum overall length of $112\frac{3}{4}$ in. The sections

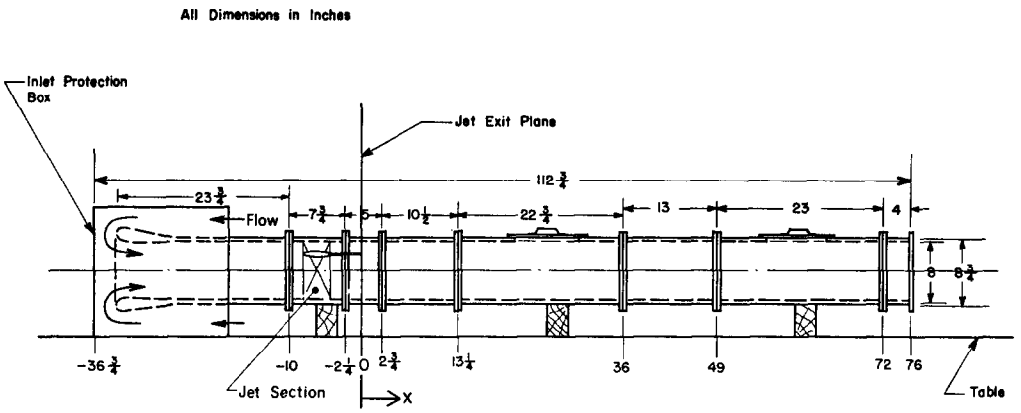

Fig. 1. Scale layout of model wind tunnel.

are made of either wood or Plexiglass and all interior wood surfaces are painted with enamel to minimize wall friction. The tunnel intake is isolated from its surroundings by a symmetrical box (Fig. 1). The use of this device was necessitated by the small size of the tunnel and its consequent susceptibility to the disturbing effects of external flows. That is, quite significant velocity fluctuations were observed to result from air currents caused by such things as traffic within several feet of the tunnel entrance, laboratory heating fans and the like. These fluctuations appeared to be associated primarily with intermittent flow separation at the inlet, which caused a periodic "surging" of the flow and fairly large variations in the mean velocities obtained both upstream and downstream of the jets. The use of a protective box over the inlet was found to be the best method of preventing these variations from occurring and although it resulted in larger turbulence levels upstream of the jets, extensive measurements showed that it had no significant effect on the turbulence characteristics obtained downstream of the jets. Static pressure readings in the tunnel were obtained by averaging the values given by a pair of taps, one located in each side wall of the tunnel, at various planes along its centreline. A scale layout of the tunnel is given in Fig. 1 and Fig. 2 is a photograph of the complete apparatus.

The jet section of the tunnel (Fig. 3) consists of eight horizontal symmetrical aluminum airfoils each having a maximum thickness of 0·5 in. and a chord of 2.5 in. These airfoils contain brass tubes which enter them through the side walls of the tunnel and which then bend downstream to emerge from the trailing edge of the airfoils. There are eight tubes leaving each airfoil and each of these extends to a distance of $5\frac{1}{4}$ in. downstream of the trailing edge, thus determining the position of the jet exit plane. Each tube has an inside diameter of 0.245 in. and is tapered to a sharp edge at its exit, such that the secondary-to-primary area ratio in the jet exit plane is $A_s/A_j = 20$. The nominal spacing between all adjacent jets is 1 in. Hence the jet grid consists of an 8 × 8 array of jets with a "mesh length" of 1 in. and the distance between any jet adjacent to a tunnel wall and the wall is $\frac{1}{2}$ in.

Primary air is supplied to the jets by a centrifugal blower. The total output of this blower can be controlled by a simple slide valve located over its inlet for the purpose of changing the overall velocity scale of the flow. Air from the blower is fed to two large pipes which act as plenum chambers. From each of these pipes, 32 independent air lines are connected to the brass jet tubes at the side of the tunnel jet section. A simple gate valve in each line

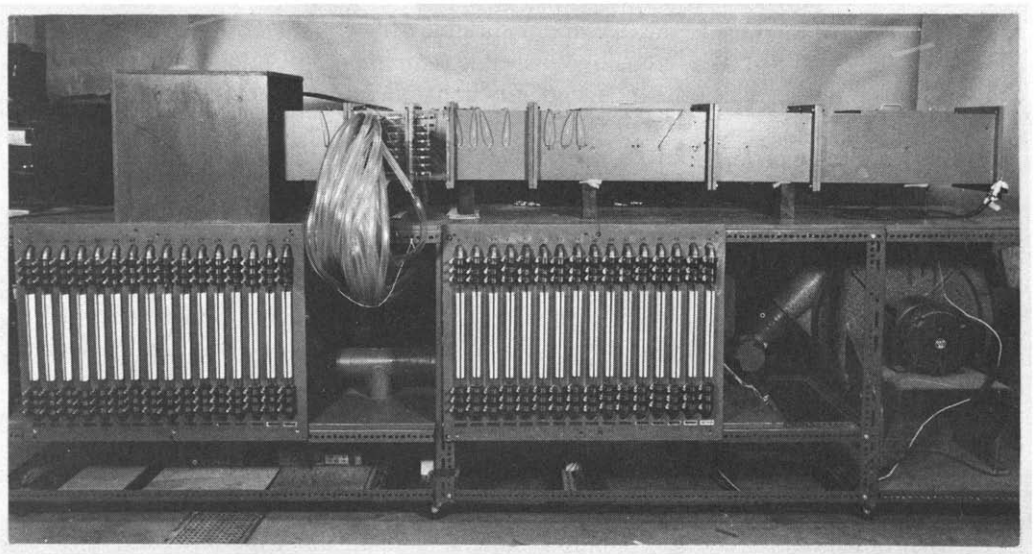

Fig. 2. Model wind tunnel.

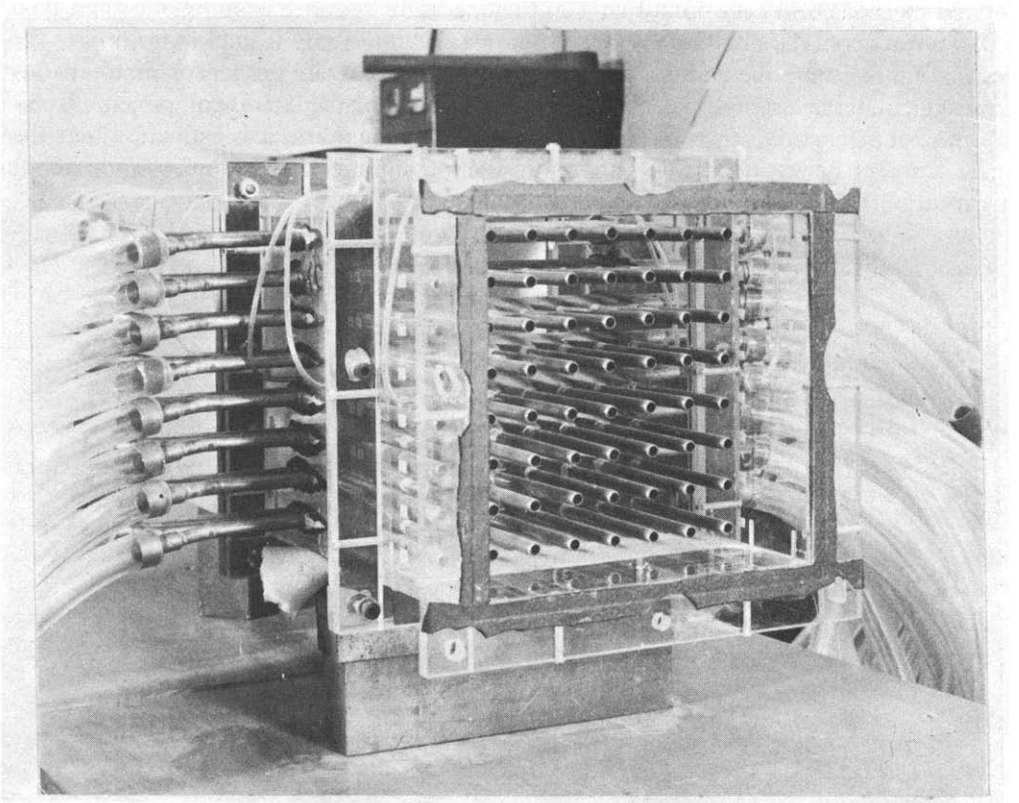

Fig. 3. Wind tunnel jet grid section.

allows variation of the flow in the line and a variable-area rotameter (Fischer and Porter Model 10A1027A) allows measurement of its value. This air supply system permits the velocity of any jet in the grid to be independently controlled to an accuracy of 2.7 per cent at maximum flow (200 ft s^{-1}) and 6.3 per cent at minimum flow (20 ft s^{-1}).

The positioning of probes in the tunnel was performed in the present experiment in two ways depending on the accuracy required. In one method the probe was mounted at right angles to a simple $\frac{1}{4}$ in. rod which protruded through the tunnel walls and which could be slid through them to move the probe either horizontally or vertically in any given plane. Probe position was then measured directly with a steel rule. This method was used for the bulk of the velocity profile measurements, and the error in positioning the probe to any location is estimated at about 0.05 in. For more accurate probe positioning, such as that required for two-point correlation measurements, a motorized, two-directional traversing rig was used and net displacements of the probes from a given initial point could be obtained to an accuracy of better than 0.01 in.

2.2 *Instrumentation and measurement techniques*

The instrumentation and data handling systems used in this experiment are outlined briefly in the following paragraphs. Complete details of the calibration procedures, system checkouts, etc. can be found in Teunissen (1972).

All turbulent flow velocity measurements made in this experiment were obtained with four channels of DISA type 55D01 constant temperature hot wire anemometers and type 55D10 linearizers. The hot wire probes used are DISA type 55E30 single wire probes for the longitudinal component and type 55A38 miniature cross-wire probes for simultaneous measurement of the longitudinal and either of the vertical or the lateral components. Temperature compensation was used throughout the experiment and it is estimated that the experimental error was about 2–3 per cent in the u-component measurements and about 5 per cent in the v- and w-component measurements.

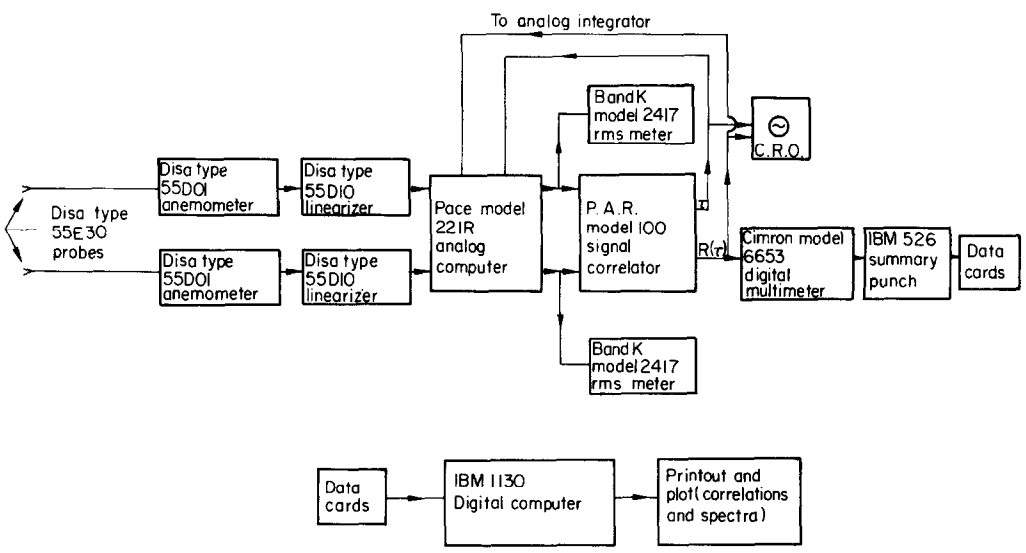

Fig. 4. Schematic layout of data handling system.

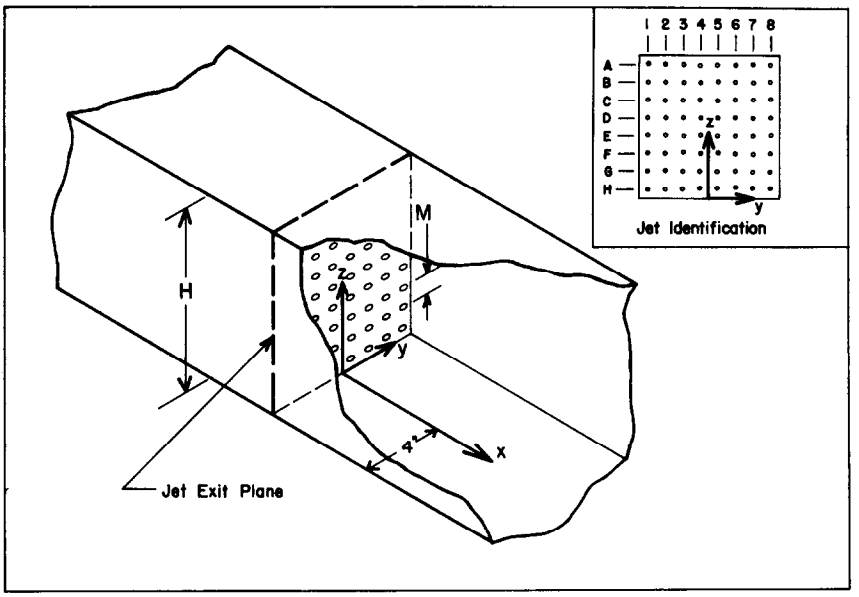

Fig. 5. Definition of coordinate system.

Manipulation of the linearized hot wire anemometer signals to obtain desired outputs was performed on a PACE model 221R analog computer. Autocorrelations and cross-correlations of the velocity components were obtained using a Princeton Applied Research Model 100 signal correlator. A Cimron Model 6480 Data Logging System and an IBM 526 Summary Punch interfaced with this correlator were used to punch the correlations on data cards. An IBM 1130 digital computer was then used to non-dimensionalize and plot these correlations, as well as to Fourier transform them to obtain power and cross-spectral densities. The complete PAR/526 system was originally devised by Surry (1969) and a schematic diagram of the system, including the hot wire instrumentation, is shown in Fig. 4. The statistical variability of spectral estimates obtained using this system was in all cases less than 5 per cent.

Root-mean-square values of the velocity components were obtained using two Bruel and Kjaer Model 2417 random noise voltmeters. These instruments provide RMS values to an accuracy of 1 per cent of full scale deflection for any input signal over the range of frequencies from 0.8 Hz (-3 dB) to 20 kHz.

Finally, mean products for any two velocity components were obtained as zero-time-delay cross-correlations using the signal correlator. In order to obtain these products from this instrument, it was necessary to use very small values of time delay and this ensures that the statistical variability of these results was negligibly small.

The location of the coordinate axes used throughout this paper is shown in Fig. 5, together with the jet labelling system adopted.

3. RESULTS FOR UNIFORM FLOW

3.1 *Flow characteristics*

Initial investigation into the capabilities of the multiple-jet tunnel was performed with all jets in the grid set to the same velocity (180 ft s^{-1}). Profiles of mean velocity and longitudinal component turbulence intensity were obtained on vertical axes ($y = 0$) at various

distances from the jet exit plane, with the result that it was no longer possible to identify the presence of individual jets beyond about 16 in. or $2H$ downstream of this plane. In addition, static pressure measurements along the length of the tunnel showed that the "pumping" action of the primary jets, as evidenced by a large pressure rise downstream of them, ceased to be significant beyond 1.5–2 H from the jets. It was therefore concluded that the jet mixing process immediately downstream of the jets is essentially completed within a distance of about 2 H (16 M) from them and that a potential test section for a tunnel of this type can be located anywhere downstream of this point.

The general characteristics of the turbulent flow produced in the tunnel with all jets set to the same velocity were found to be similar to those of the flow produced behind conventional bi-planar grids of rods. In Fig. 6 the turbulence intensity for the longitudinal component along the tunnel centreline is seen to decay in the downstream direction from an

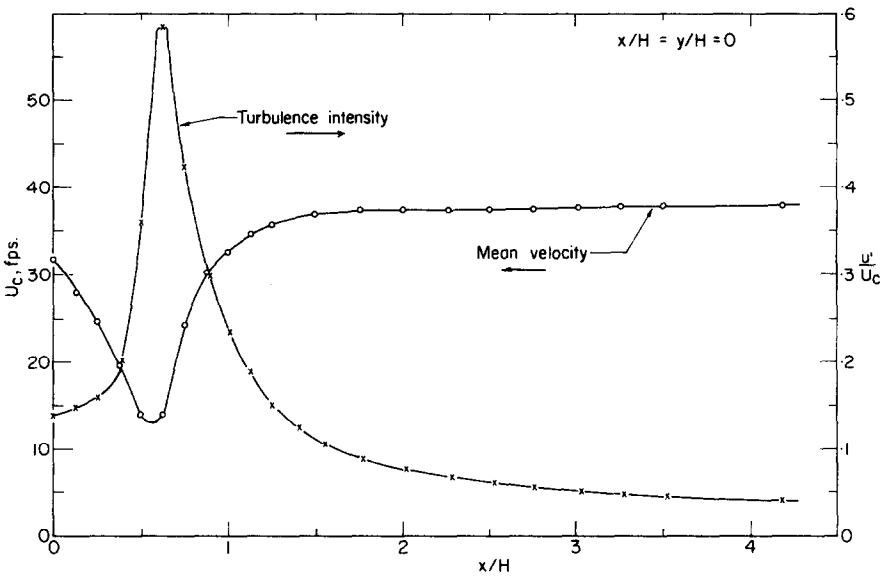

Fig. 6. Centreline flow properties in uniform flow. All jets set to $U_j = 180\,\text{ft}\,\text{s}^{-1}$.

effective origin at $x/H \sim 0.6$ and this decay is similar to that observed behind grids of rods (Batchelor and Townsend, 1948; Baines and Peterson, 1951). We see here also that the mean velocity leveled off by $x/H \sim 1.5$, beyond which it increased gradually due to the growth of wall boundary layers in the tunnel. Measurements taken in the plane $x/H = 2.5$ indicated good homogeneity of the various turbulence characteristics across the flow. Turbulence intensity levels for the v- and w-components in this plane were virtually equal while that of the u-component was about 15 per cent larger. Integral scale measurements showed that $L_v \sim L_w \sim 0.2$–$0.25\,M$ and that L_u was roughly twice this value, as it would be in a truly homogeneous flow. In general, then, the flow produced beyond the jet mixing region was a uniform, nearly homogeneous turbulent flow which was decaying slowly in the downstream direction.

The effect of fine adjustment of the jet velocities on the characteristics of the flow is shown in Fig. 7. With all jets set to the same velocity, the maximum variation of the mean

velocity across the tunnel at $x/H = 2.5$ is seen in Fig. 7b to have been about 5 per cent. This variation is attributed primarily to physical non-uniformities of the jet grid arising from the difficulty in its construction as a result of the generally small scale of the experiment. By slightly adjusting the velocities of the appropriate jets in the grid, it was found possible to reduce this variation to less than 1 per cent. This jet adjustment was done by an iterative technique. That is, it was found in general that the velocity at any height in the tunnel is dependent on the jet velocity in the grid row corresponding to that height and also on that of the rows immediately above and below this row. This velocity is, however, relatively insensitive to jet velocity changes in other rows. Consequently, in order to

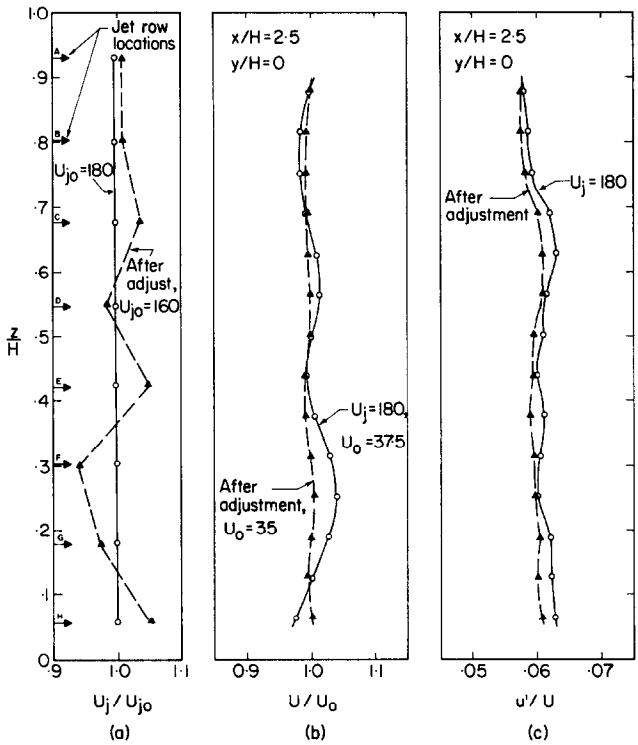

Fig. 7. Effect of fine adjustment of jets in uniform flow.

obtain a desired velocity profile in a fixed plane in the mixed-flow region of the tunnel, a hot wire probe was placed at one of eight heights on a vertical axis in the plane, and the velocity of all the jets in the row corresponding to this height were then adjusted until the desired velocity was obtained at the probe location. This adjustment was then performed for the other seven heights on the axis, and the entire procedure was repeated iteratively until the desired velocity profile was obtained. Only two iterations were necessary to achieve the profile improvement displayed in Fig. 7b, although it must be remembered that the procedure would have to be repeated in the horizontal direction, and at various heights, in order to obtain improved uniformity across the entire flow. The procedure is in general, however, not very tedious for reasonable desired velocity profiles. The results in Fig. 7a show the jet input profiles before and after the fine jet adjustment, i.e. the velocity

to which each row of jets had to be set in order to produce the desired result. Finally, the curves in Fig. 7c indicate that although there was significant improvement in the mean velocity variation across the tunnel, fine adjustment of the jet velocities did not greatly improve the uniformity of the turbulence intensity profiles in this plane. Consequently it was concluded that uniformity of the jet grid itself should be fairly important objective in building a full-size version of the present tunnel.

3.2 *Tunnel performance*

The mean velocity obtained in the mixed-flow region of the jet tunnel can be predicted in terms of the primary jet velocity with the aid of the continuity and momentum equations and a few simplifying assumptions. This simple ejector theory is outlined in Teunissen (1972), and it predicted that for the geometry used in the present wind tunnel, the ratios of the average entrained flow (i.e. upstream of jets) and mixed flow velocities to the primary jet velocity should be, respectively, $U_e/U_i = 0{\cdot}23$ and $U_m/U_j = 0.27$. When some account was made for the loss of energy due to friction based on experimentally measured pressure losses, the above ratios were reduced to 0.17 and 0.21, respectively. Experimental measurements of these quantities were made with all jets set to 180 ft s^{-1} and yielded values which agree with the reduced ratios within less than 3 per cent. These ratios, together with the appropriate dimensions of any proposed tunnel, are sufficient to permit determination of the total input power required for a tunnel of this type.

4. PLANETARY BOUNDARY LAYER SIMULATION

4.1 *Planetary layer characteristics*

The extreme complexity of the flow in the planetary boundary layer and the difficulty in making controlled measurements of its characteristics has resulted in a fairly large degree of scatter in the data obtained from different sources in many cases. However, certain trends and relationships are fairly well established. The author has reviewed much of the data available (Teunissen, 1970) and some of the results of this review are outlined in this section. We are concerned here only with planetary flows which are neutrally stable and in which the effects of Coriolis accelerations may be neglected. This somewhat restricted class of flows is of limited usefulness in studying certain problems such as the dispersal of pollutants and the like, where thermal stability and directional effects may be of major concern. There is, however, a large class of instances in which it is not at all unreasonable to neglect these effects, particularly in the case of high mean wind speeds and at moderate heights above the surface (Davenport, 1965; Harris, 1968).

Based on the above assumptions, then, and also assuming that the gross features of the terrain are reasonably uniform, the variation of mean velocity with height through the planetary layer may be adequately represented by the so-called power profile,

$$U/U_\delta = (z/\delta)^\alpha. \tag{1}$$

In the surface layer alone, where shear stress is assumed constant at all heights, and which usually extends to a height of about 0.2 δ, the mean velocity may be expressed by

$$U/U_\tau = 2{\cdot}5 \ln (z/z_0).$$

The parameters α, δ and z_0 depend on the roughness of the surface and some typical values suggested by Davenport (1965) are given in Table 1.

Table 1

Surface	α	δ (ft)	z_0 (ft)
Flat open country	0.16	900	0.1
Woodland forest	0.28	1300	1
Urban	0.35	1600	3.5

Turbulence intensities in the surface layer are given roughly by

$$u'/U = 1/\ln(z/z_0) \tag{2a}$$

$$v'/U = 0{\cdot}8/\ln(z/z_0) \tag{2b}$$

and

$$w'/U = 0{\cdot}5/\ln(z/z_0) \tag{2c}$$

so that the ratio of the component intensities is $u'/v'/w' \sim 1/0.8/0.5$ in this region. These turbulence levels all decrease toward zero above the surface layer. The Reynolds stresses $\overline{uv}$ and $\overline{vw}$ are assumed to be zero, while the constant value of $\overline{uw}$ in the surface layer is given by $\overline{uw}/u'w' \approx -0.3$. The power spectral densities of the velocity components are best fitted by the von Kármán equations for isotropic turbulence. That is, for the longitudinal component,

$$\frac{k\,\phi_u(k)}{\overline{u^2}} = \frac{4\,k\,L_u}{[1 + 70.7\,(L_u k)^2]^{5/6}} \tag{3}$$

while for the lateral component,

$$\frac{k\,\phi_v(k)}{\overline{v^2}} = 4\,k\,L_v\left\{\frac{1 + 188.4\,(2\,L_v k)^2}{[1 + 70.7\,(2\,L_v k)^2]^{1\,1/6}}\right\} \tag{4}$$

and the expression for the vertical component is similar to that for the lateral component. Finally, the integral scales of the turbulence are given roughly by

$$L_u \approx 20\sqrt{z}, L_v \approx L_w \approx 0.4\,z. \tag{5}$$

It must be emphasized here that while the velocity profile relations given above have been fairly well verified for the atmosphere, the exact values of the parameters, as well as the other relations above, are merely best estimates, and actual measured values obtained in the atmosphere often differ considerably from these estimates.

In Fig. 8, data for the variation of the intensity of the longitudinal turbulence component through both the actual planetary boundary layer and wind tunnel simulations of it are summarized. These data have been obtained from many sources and the values suggested by equation (2a) for various surface conditions are shown for comparison. It is seen that while the data do display considerable scatter as mentioned above, distinct trends are certainly established for similar values of α. The integral scale profiles through the planetary layer as predicted by equation (5) are also shown in Fig. 8, together with some data obtained in a boundary layer wind tunnel. The values $L_u/\delta = 0.42$ and $L_w/\delta = 0.22$ were taken as representative atmospheric values at $z/\delta = 0.57$ and were used for locating the appropriate von Kármán spectral model on the frequency axis when comparing atmospheric and experimental results (Sections 4.5, 4.6).

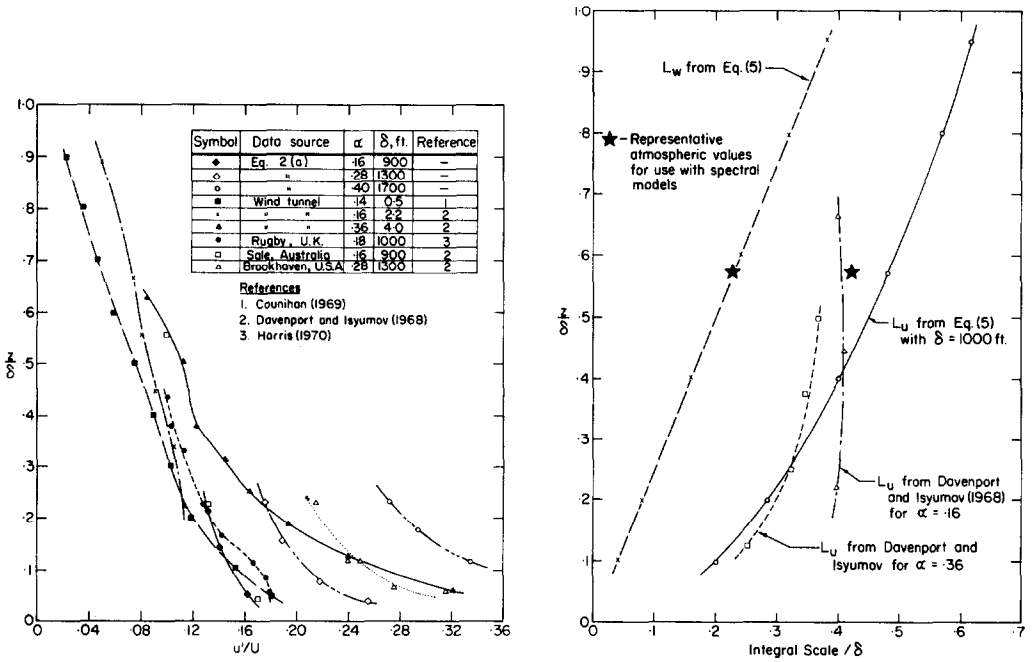

Fig. 8. Turbulence intensity and integral scale characteristics in wind tunnel and planetary flows.

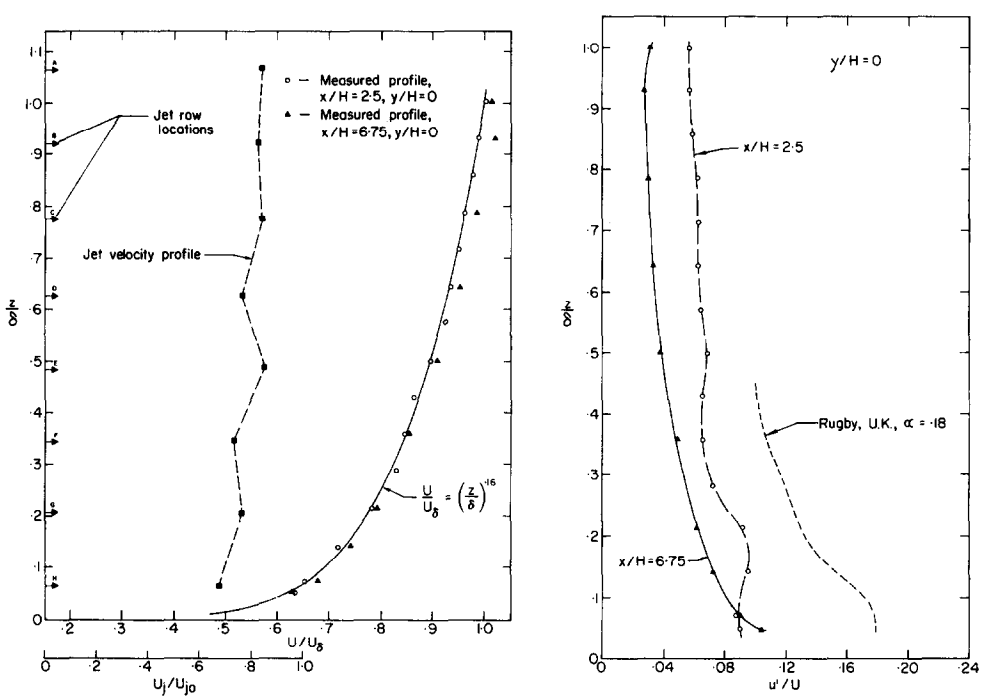

Fig. 9. Mean velocity and turbulence intensity profiles in flow set up to obtain $\alpha = 0.16$ at $x/H = 2.5$ with smooth tunnel floor.

4.2 *Flows with smooth tunnel floor*

In producing simulated planetary flows in the jet tunnel, the velocity profiles given by equation (1) were the ultimate objectives. That is, the goal was to obtain, by adjustment of the jet velocities, a flow possessing a power-law mean velocity profile with a particular value of α at a specific plane in the mixed-flow region of the tunnel. Once this flow was established, investigation of its turbulence characteristics could be performed. It was felt initially that setting the jet velocities themselves to obey a power-law profile might result in a similar flow downstream. Unfortunately, however, this approach was found to be unsuccessful, presumably because of jet interaction and tunnel wall effects, and consequently the reverse procedure was adopted. That is, a probe was placed at various heights in the plane of interest and velocity adjustment, using the iterative technique described in Section 3.1, was performed until the desired velocity profile was obtained. This was done initially in only the vertical direction, since lateral uniformity of the flows was found to be reasonable and any improvement by further jet adjustment in the horizontal direction was not necessary.

The results of setting up a flow with a power-law mean velocity profile having $\alpha = 0.16$ at $x/H = 2.5$ with no roughness on the tunnel floor are shown in Fig. 9. The agreement of the experimental mean velocity data with the desired curve is seen to be excellent and is typical of that obtained for differing values of α at any plane beyond $x/H = 2$. This degree of agreement was achieved in general after only 3 or 4 iterations of jet velocity adjustment. It can also be seen that there was little decay of the velocity profile shape in the downstream direction, although its magnitude increased slightly due to the growth of wall boundary layers. The jet velocity profile required to obtain this flow is seen to be quite uniform, with local bulges being attributed to the aforementioned non-uniformities in the jet grid section of the tunnel. The turbulence intensities measured in the flow were rather disappointing, however, at least insofar as planetary boundary layer simulation is concerned. The magnitude of the turbulence levels obtained was far below that of comparable planetary flows and in addition, a fairly large decay of the turbulence in the downstream direction can be observed.

Further results for downstream variation of the flow properties are presented in Fig. 10. It is seen here that the integral scale increased in the downstream direction, as we would expect, but was well below the target value of $L_u/\delta = 0.42$ suggested in Section 4.1 for this height. In addition, spectral measurements showed a not unreasonable agreement of the measured power spectra with the shape of the von Kármán model, but the entire spectrum was shifted toward higher frequencies as a result of the small scale of the turbulence.

4.3 *Effects of surface roughness*

The foregoing results indicate that while the jet tunnel was found to be capable of producing virtually any mean velocity profile at any plane in the mixed-flow region, insufficient turbulence for our purposes was produced by the jet mixing process, and some other method would be needed in order to raise the turbulence levels to those found in atmospheric flows. As a first attempt to solve this problem, simulated surface roughness was placed on the floor of the tunnel, beginning at or near the jet exit plane and continuing to the tunnel exit. This roughness serves three basic purposes. First, it ensures that the simulated flow is aerodynamically rough, as is the atmospheric flow in virtually all instances. This is a requirement for similarity of the flows (Sundaram *et al.*, 1970) in that

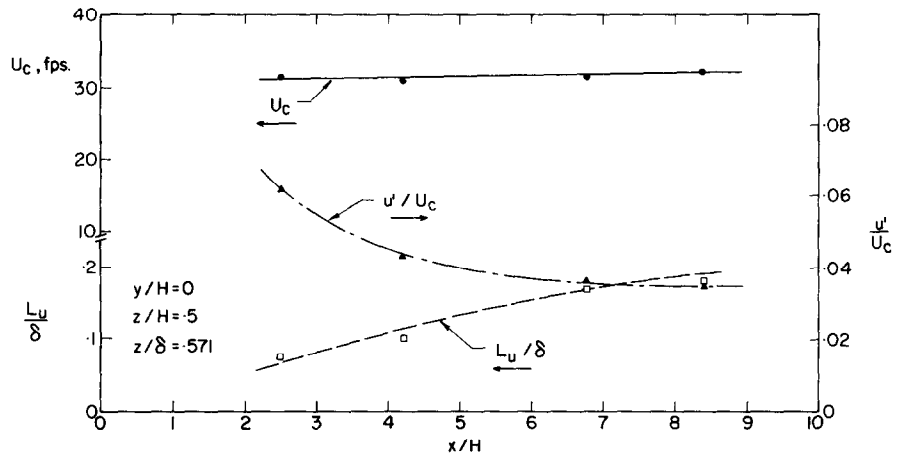

Fig. 10. Centreline flow characteristics for flow with $\alpha = 0.16$ velocity profile set at $x/H = 2.5$ with smooth tunnel floor.

it will in general minimize the effects of viscosity in the laboratory flow and thereby reduce Reynolds number dependence. That is, unless the simulation is attempted on too small a scale, aerodynamic roughness of the flow will tend to forestall the rapid falloff at the high frequency end of typical power spectral density curves, which is indicative of the viscous dissipation of energy, and a significant inertial subrange should be obtained in the spectra. Secondly, the roughness should prevent velocity profiles from becoming more uniform with increasing distance downstream of the jets. This phenomenon is not observed in Fig. 9 because of the small value of α used for this flow; however, for $\alpha = 0.25$ and 0.35, a significant decay, in the form of increasing velocities near the tunnel floor, was observed from the plane $x/H = 2.5$ to $x/H = 6.75$ in the absence of surface roughness. Thirdly, the additional shear stresses produced by the roughness should increase turbulence production near the tunnel floor, i.e. in the same region where it primarily occurs in any natural boundary layer, including the planetary layer—and it was hoped that this would increase the turbulence levels to the desired values.

The simulated surface roughness used in the present experiment consists of baseplates from a "LEGO" construction set for flows with $\alpha = 0.16$, sheets of $\frac{1}{2}$ in. industrial expanded sheet metal for $\alpha = 0.25$ and LEGO baseplates with alternately arranged $\frac{1}{2}$ in. cylindrical "bricks" for $\alpha = 0.35$. These roughness materials were found in general to be adequate for the particular flows desired.

Typical results of adding the appropriate roughness to the tunnel floor are shown in Figs. 11–13. In Fig. 11, the results of producing a flow with a power-law mean velocity profile having $\alpha = 0.25$ at $x/H = 2.5$ are presented. Excellent agreement with the desired velocity profile was again achieved, and although the magnitude of the curve increased in the downstream direction due to boundary layer growth, there was little change in its shape. It was possible to obtain almost exactly the desired velocity profile in the plane $x/H = 6.75$ simply by using this plane in setting the jet velocities. This is shown in Fig. 12 where it is also evident that little change occurred downstream of this plane in spite of the fact that a very distorted mean velocity profile existed at $x/H = 2.5$. Notice also that in both of these cases, the required jet velocity profile was considerably more distorted than that needed to produce the flow of Fig. 9, in which the tunnel floor was smooth. It

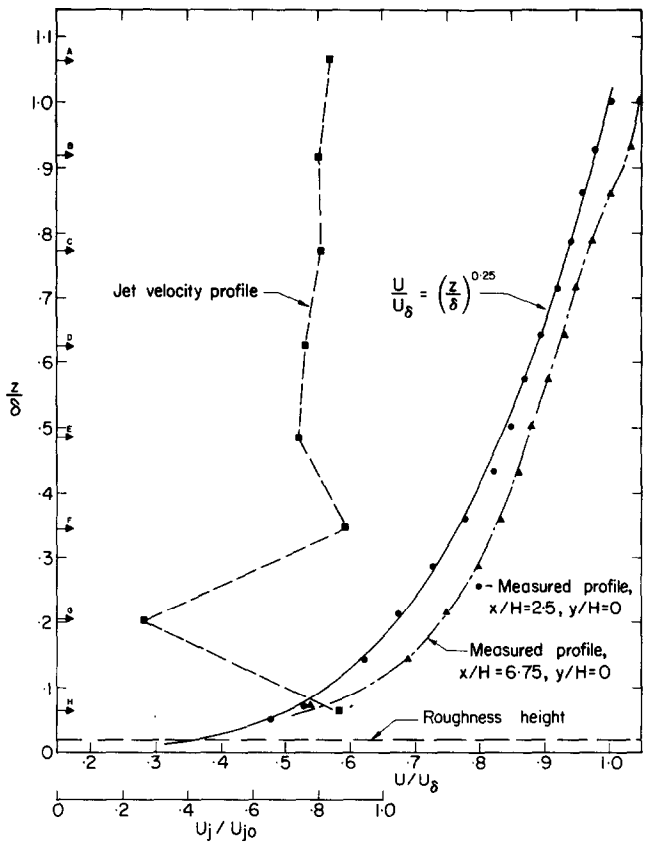

Fig. 11. Results of setting $\alpha = 0.25$ velocity profile at $x/H = 2.5$ with roughness beginning at $x/H = 0$.

was found in general that the shape of the jet velocity profile for any flow depends on the particular power-law profile chosen (i.e. α), the plane in which this profile is set, the presence or absence of surface roughness and the distance downstream of the jets at which this roughness is begun. For example, in the cases where the mean velocity profile was set up at $x/H = 2.5$, a considerably more uniform (and therefore more easily set up) jet velocity profile was required when the surface roughness was begun at $x/H = 2.0$ rather than at $x/H = 0$. In cases when this profile was set up at $x/H = 6.75$, however, (e.g. Fig. 12), surface roughness location had a much smaller influence on the necessary jet velocity profile.

As for the turbulence levels found in the above flows, the results are generally summarized in Fig. 13. It is clearly seen that although the roughness raised the turbulence intensity in the flow near the bottom of the tunnel, it had virtually no effect above this region. The turbulence level generally remained below that found in a planetary flow with $\alpha = 0.16$, and far below that in a planetary flow with a more comparable value of $\alpha = 0.28$. The ineffectiveness of the roughness at higher levels was not entirely unexpected and arose from the fact that the roughness on the tunnel floor can significantly alter the turbulence characteristics only in its own natural boundary layer. In this layer the turbulent diffusion of energy from the surface to the outer regions of the layer is taking place, but above it no comparable mechanism exists. Similar results have been encountered by Templin (1969).

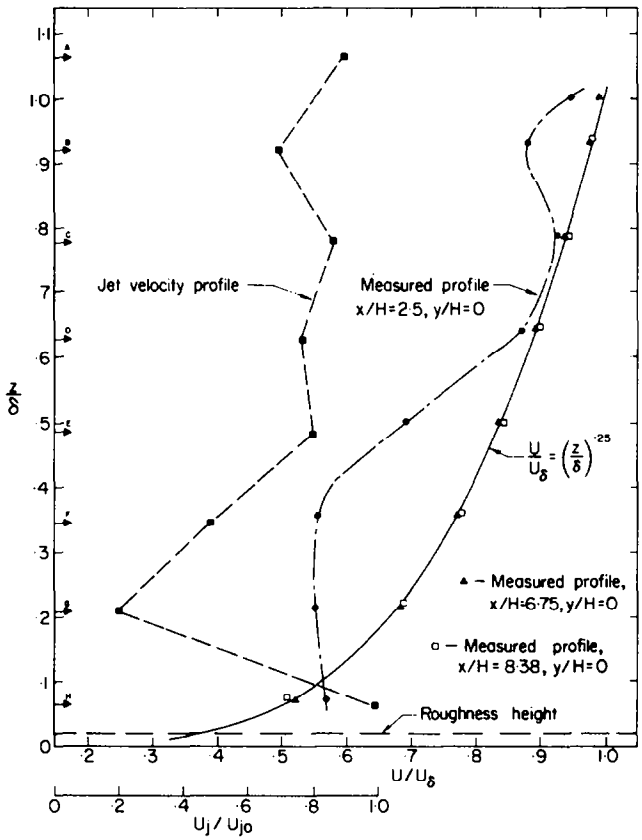

Fig. 12. Results of setting $\alpha = 0.25$ velocity profile at $x/H = 6.75$ with roughness beginning at $x/H = 2.0$.

Fig. 13 indicates that at $x/H = 6.75$, the natural boundary layer had a thickness of about $0.3\ \delta$ in this flow and above this height, roughness effects were minimal. It was therefore concluded that while surface roughness could prevent the decay of velocity profiles in the downstream direction, it could not add sufficient turbulence for our purposes and other means would be required.

As mentioned above, the velocity profile required at the jets in order to obtain a particular flow is a function of the roughness used, its location, the value of α and the plane in which the flow profile is set. Presumably the shape of the jet profile is independent of the selected value of U_δ, although the magnitude of the curve as a whole should depend on this value. In order to determine if the jet profile for a particular set of the above parameters is unique or whether some different combination of jet velocities could produce the same flow profile, a particular flow was created twice by successive iterations from two widely different initial jet profiles. That is, for the flow shown in Fig. 11, the mean velocity profile was first obtained with all jets set initially to the same velocity, and the jet profile shown was the ultimate result after the iteration procedure. The process was then repeated with the jets set initially to a profile that appeared as if it might be more appropriate ($\alpha \sim 0.2$) to the desired flow, and in spite of deliberate attempts to avoid it, exactly

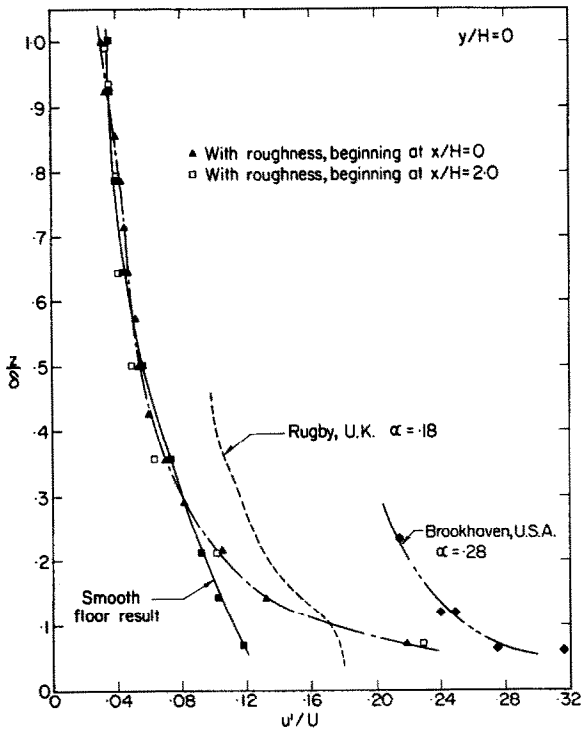

Fig. 13. Turbulence intensity profiles at $x/H = 6.75$ for $\alpha = 0.25$ velocity profiles set at $x/H = 2.5$.

the same (within a few per cent) jet velocity profile, including the very low value of row *G*, was inevitably obtained. While a test of this nature can of course be absolutely conclusive only if an infinite number of starting jet profiles are investigated, it would seem that if the above initial profile still lead to the same oddly-shaped end result of Fig. 11, then so probably would any other initial profile. Thus the jet velocity profiles required for any particular flow are indeed considered to be unique.

One would of course expect that the flows created in the tunnel for a particular configuration should be repeatable, particularly in view of the results discussed in the preceding paragraph. That is, for a given case of roughness and power-law profile, resetting of the jets to the values originally determined for this case should produce the same flow downstream of the jets. It was found throughout this experiment that the flows were indeed repeatable, with the velocities obtained at the particular plane in question being the same as those originally produced to within the accuracy of their measurement.

4.4 *Effects of other turbulence-producing methods*

Returning now to the problem of increasing the turbulence levels obtained in the tunnel, several different approaches were tried. In one of them, alternate columns of jets were set to velocities 10 per cent above and 10 per cent below the nominal values required to produce a particular flow. The reasoning behind this was that beyond the mixing region, the velocity profile should regain horizontal uniformity since the average flow from the jets in a particular row would be the same as it was originally. However, due to the large differences in adjacent jet velocities, the shears (i.e. velocity gradients) in the mixing region

would be considerably increased. Thus the turbulence levels here would be increased via turbulence production terms (e.g. $\overline{uw}\,\partial u/\partial z$) and hopefully this increase would be felt along the entire length of the tunnel.

Investigation of the flow produced with the jets set in this manner showed that reasonable horizontal uniformity was indeed obtained as far upstream as $x/H = 2.5$. However, while the turbulence levels in the mixing region were somewhat higher than previously, the intensities at $x/H = 2.5$ were only slightly larger and at $x/H = 6.75$ there was in fact no significant change. As a further step, similar alternation of the velocities of the jets in each column was also tried, but again there was virtually no change in the flow beyond $x/H = 2.5$. This may have resulted from the small scale of the turbulence in the jet-mixing region and from the fact that the relative difference in velocity between the jets and the entrained flow was not so greatly altered by only a 10 per cent variation in the jet velocities; however, larger variations could not be obtained for the present flows. Thus it was concluded that any increase in turbulence resulting from increased shear between the flows from adjacent jets and the secondary, entrained flow is in general not significant beyond the jet-mixing region, at least for this range of velocity variations.

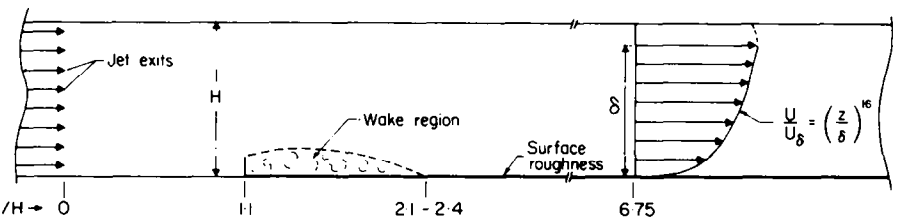

Fig. 14. Typical tunnel configuration with barrier and simulated surface roughness.

The effectiveness of a set of vortex generators in increasing turbulence in the flow by the addition of a streamwise vorticity component was also investigated. Devices of this type could presumably also assist in the distribution of turbulent energy from the region near the tunnel floor into the upper regions of the flow. Simple flat plates were placed at differing angles across the floor and roof of the tunnel at $x/H \sim 2$ and the flow characteristics were investigated at $x/H = 6.75$. It was found in general that only a very small increase in turbulence intensity was produced in the flow, while the scale of this turbulence was considerably smaller than without these devices. In addition, it was found to be extremely difficult to produce desired velocity profiles in the tunnel as a result of the greatly increased coupling between the mixed-flow velocity at any point and the velocity of the jets in the grid. Consequently, attempts to raise turbulence levels with these devices were abandoned.

In many of the planetary flow simulations performed by other investigators (e.g. Counihan, 1969; Davenport and Isyumov, 1968) use was made of a flat barrier-plate placed horizontally across the floor of the wind tunnel to "trip" the flow. Because of the large amounts of wake turbulence that such barriers produce, their effectiveness in raising the turbulence intensities in the flows produced in the jet tunnel was investigated. This wake turbulence is also of relatively large scale and it was therefore expected to improve the integral scale characteristics of the mixed flow in the tunnel. Aluminum plates 1 and 1.5 in. high were used to obtain flows possessing a power-law mean velocity profile with $\alpha = 0.16$ at $x/H = 6.75$. Figure 14 shows a typical configuration for their use. In Fig. 15 it is clearly seen that

large differences in turbulence intensity over the entire height of the flow were achieved in the plane $x/H = 6.75$ by use of these barriers. It is emphasized that for all three curves shown in this figure, the corresponding mean velocity profiles followed the same $\alpha = 0.16$ power-law profile very well, as typified by the results shown in Fig. 16 for one case. It is also interesting to note here that the jet velocity profile required to produce the desired flow with the 1 in. barrier was quite uniform in spite of the presence of the barrier; for the 1.5 in. barrier, however, there was considerably more distortion in the jet profile, as

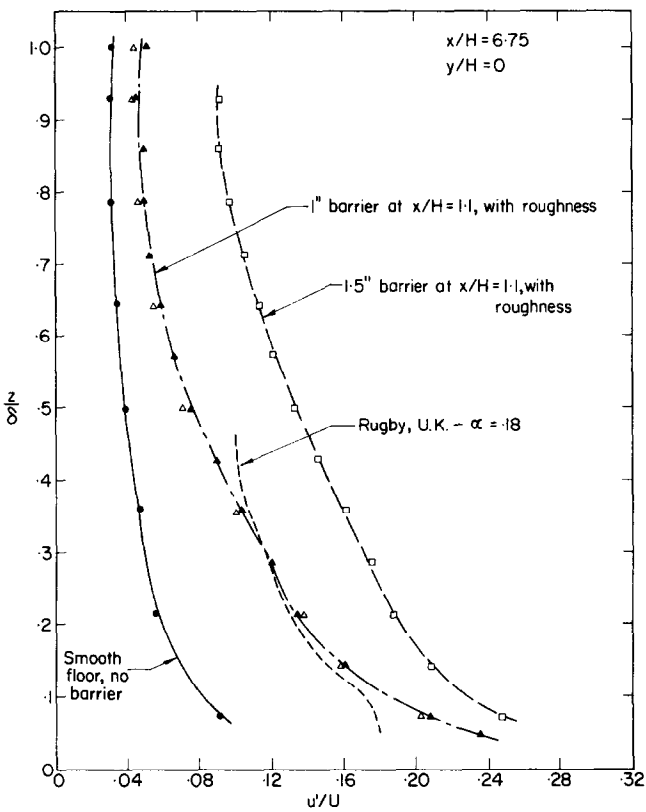

Fig. 15. Effects of barriers on turbulence intensity profiles for flows with $\alpha = 0.16$ velocity profile set at $x/H = 6.75$.

one would expect. It is seen from these results, then, that the barriers allow variation of the turbulence levels in the flow while adjustment of the jet velocities enables the same velocity profiles to be simultaneously retained.

The results of Fig. 16 also indicate that a very good degree of lateral homogeneity of the flow was achieved in this plane. This was done by choosing the horizontal axis at $z/\delta = 0.57$ in the plane and performing column-by-column iterative adjustment of the jet velocities until the desired degree of uniformity was obtained. This procedure was found to be quite straightforward and was obviously very successful.

Some further barrier tests were performed to determine the effect of the location of a particular barrier on the characteristics of the flow. It was found that there is virtually no

difference in the turbulence in the flow when the 1 in. barrier is placed at 2 H downstream of the jets rather than at 1.1 H. A test with the barrier upstream of the jets ($x/H = -1.75$) showed, however, that it had no significant effect at all on the turbulence in the mixed-flow region downstream of the jets and the profile here was the same as if no barrier were present. Thus the region $x/H \sim 1$ is likely the best location for any barrier used, since placing it closer to the jets would result in greatly increased difficulty in obtaining the desired velocity profile.

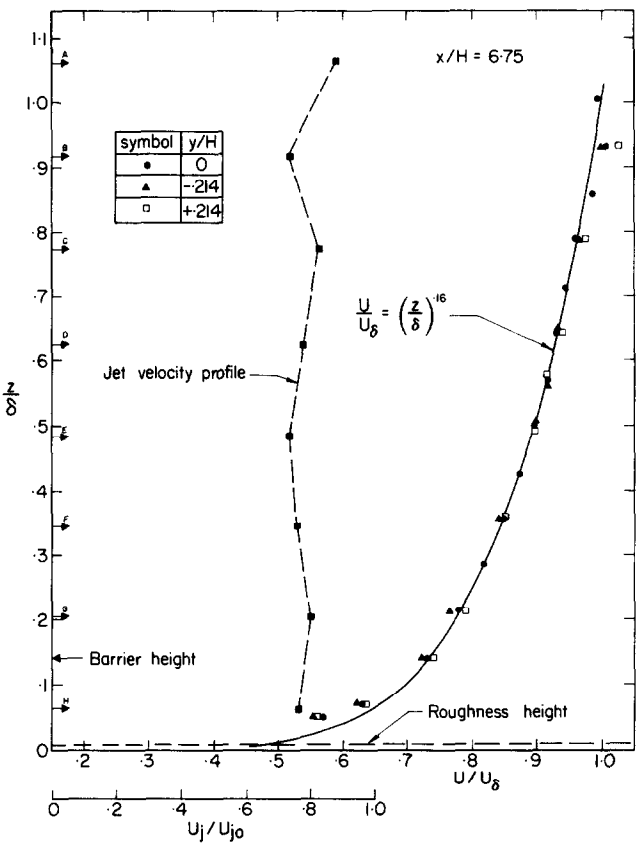

Fig. 16. Results of setting $\alpha = 0.16$ velocity profile at $x/H = 6.75$ with roughness and 1 in. barrier at $x/H = 1.1$.

4.5 *Simulated flow characteristics*—$\alpha = 0.16$

In view of the good agreement between the tunnel and planetary turbulence intensity results displayed in Fig. 15 for the case of a 1 in. barrier in the tunnel, and because of the excellent velocity profiles achieved, this particular flow was further investigated as a simulation of the planetary flow over flat, open terrain. Its development in the downstream direction is indicated by the profiles of Fig. 17. It is seen from these results that virtually all the downstream variation occurred in the bottom half of the tunnel and that the upper regions were quite stable. Little change occurred in the mean velocities beyond $x/H \sim 5.5$, while the turbulence, as expected, required a somewhat larger distance to stabilize. These

results suggest that the region $x/H \sim 6$–8 should make a reasonable test section for this type of configuration in the tunnel.

Further measurements of the characteristics of the present flow were made in the plane $x/H = 6.75$. In Fig. 18 the turbulence intensity profiles for the lateral and vertical velocity components are compared with that of the longitudinal component. These results are similar to those found in a natural turbulent boundary layer (Klebanoff, 1956) in that the component in the direction of the shear gradient was the smallest and all three components decreased toward the same value in the upper regions of the flow. At $z/\delta = 0.1$, the components were in the ratio $u'/v'/w' \sim 1/0.78/0.54$ and this compares well with the values 1/0.8/0.5 suggested in Section 4.1 for the planetary surface layer.

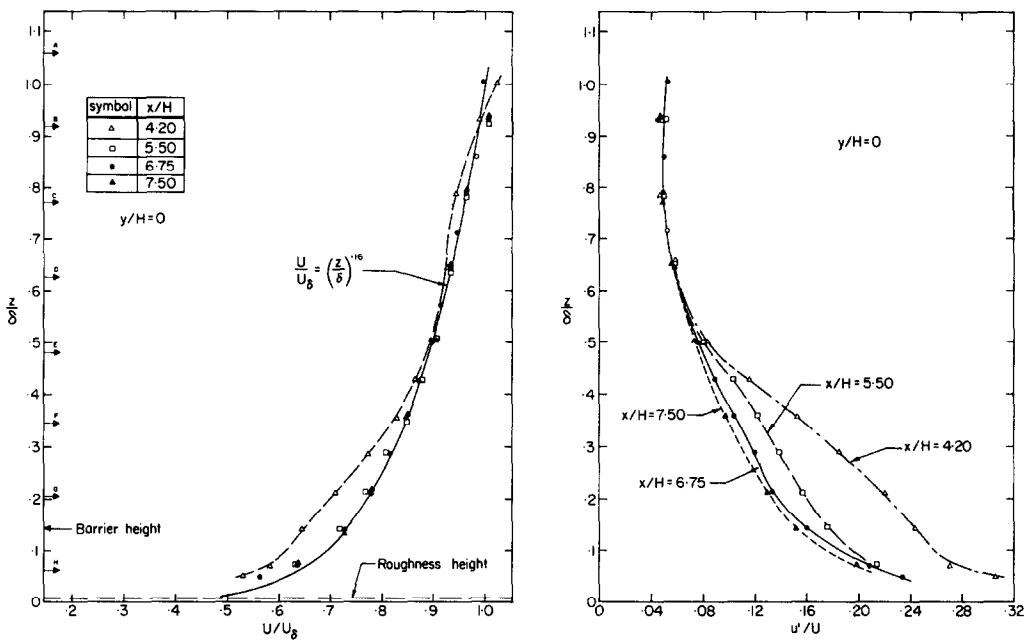

Fig. 17. Downstream variation of mean velocity and turbulence intensity profiles. Velocity profile $\alpha = 0.16$ set at $x/H = 6.75$ with roughness and 1 in. barrier.

The vertical variation of integral scales is also shown in Fig. 18. These scales were determined from the location of the peaks of the appropriate power spectral density curves along the frequency axis, on the assumption that these curves could be reasonably well fitted by the von Kármán model spectrum (Teunissen, 1972). This approach resulted in a typical scatter of about ± 15 per cent in the data measured at any point. It is seen that the use of the barrier resulted in values of L_u whose magnitudes were in fairly good agreement with suggested atmospheric values. In addition, a distinct increase in L_u with height is observed, similar to that suggested by equation (5) for the planetary layer. It must be reiterated, however, that equation (5) is merely an estimate of atmospheric scales and considerable scatter of the data about this curve is found. However, the relation is useful as an indicator of the overall magnitude and trend of the atmospheric data. As for the vertical component scale, L_w, comparison of the profile shown here with that of equation (5) indicates that rather poor simulation of this scale was achieved in the upper half of the tunnel.

It is felt that the small scales obtained here were likely due to the presence of the tunnel roof and the absence of a free stream region above the simulated boundary layer. It is noted that it should be possible, if necessary, to produce a flow in the jet tunnel that does include a free stream region; however, the properties of such a flow were not investigated in the present study (either more rows of jets or some modification of the boundary condition at the top of the flow would be required). In the lower regions of the flow, the values of L_w are seen to have been not unreasonable. Finally, the values of L_u and L_w at $x/H = 8.38$ are presented in Fig. 18 and indicate that little downstream change in these scales occurred in this section of the tunnel.

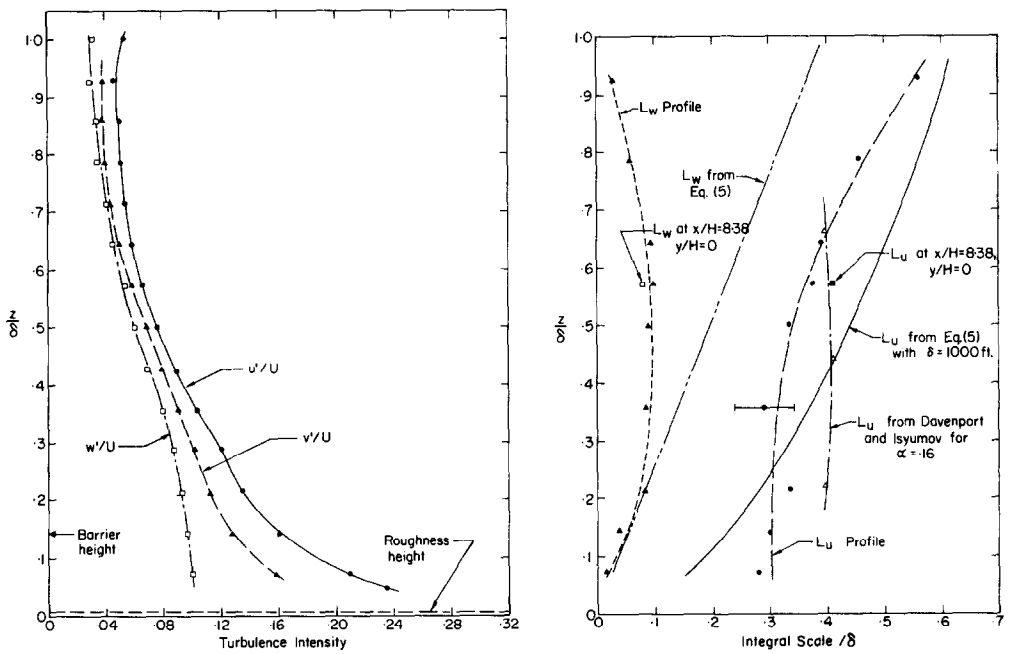

Fig. 18. Turbulence intensity and integral scale profiles at $x/H = 6.75$, $y/H = 0$. Velocity profile $\alpha = 0.16$ set at $x/H = 6.75$ with roughness and 1 in. barrier.

Typical power spectral density results are shown in Fig. 19. It is seen here that there was some deficiency in the low frequency content of the simulated flow as compared with the appropriately located von Kármán spectral model, although the general agreement of the curve shapes is not unreasonable. The rapid falloff of the experimental data at the high frequency end represents the beginning of the viscous dissipation region and is not modelled in the von Kármán spectrum. It appears in the present results, in spite of the aerodynamic roughness of the flow, only because of the small scale of the experiment, and it would be expected to be beyond the range of interest relative to the position of the spectral peak in a full-size version of this tunnel (e.g. 6 × 6 ft). Further discussion of this point can be found in Teunissen (1972) and Templin (1969). Figure 19a for the longitudinal component shows that there was little shift of the spectrum along the frequency axis with increasing distance from the jets. This indication of flow homogeneity in the longitudinal direction is equivalent to the corresponding non-variation of integral scale observed in Fig.

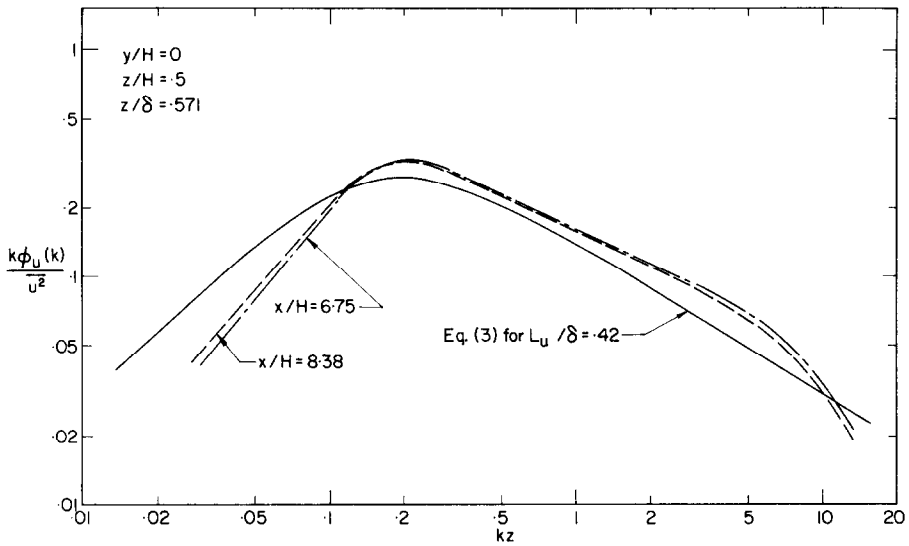

(a) Longitudinal Component

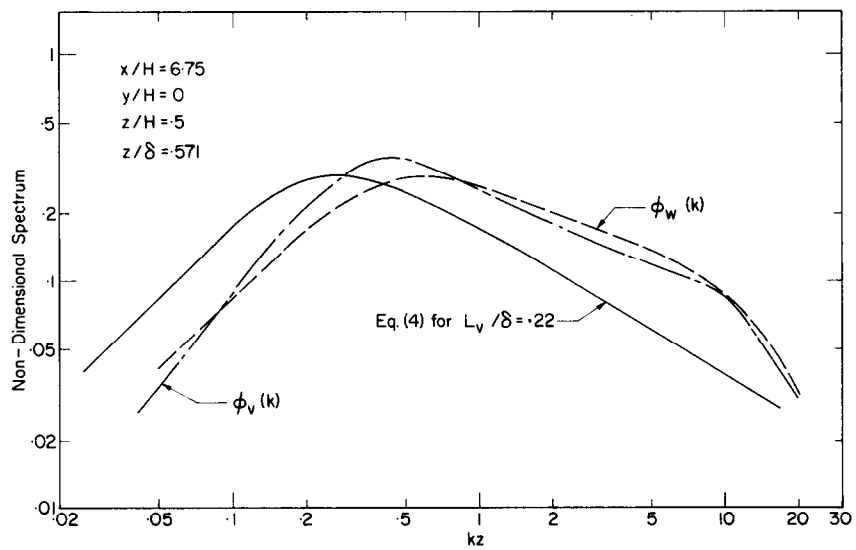

(b) Lateral and Vertical Components

Fig. 19. Power spectral density results on tunnel centreline. Velocity profile $\alpha = 0.16$ set at $x/H = 6.75$ with roughness and 1 in. barrier.

18. As for the other component spectra, Fig. 19b shows them to be located at somewhat too high a frequency, a fact which is of course synonymous with the low scales observed for these components. On the whole, the spectra obtained in this flow are considered to be reasonable simulations of those found in the atmosphere, although it is suggested that further improvement might result from alterations to the barrier.

The variation of the Reynolds stress coefficients through the simulated flow is displayed in Fig. 20. As required, the $\overline{uv}$ coefficient was quite small while the $\overline{uw}$ coefficient was fairly

constant and was not far from the value of -0.3 suggested in Section 4.1 for the planetary surface layer. The dimensional form of $\overline{uw}$ is also shown and it is seen to have decreased with height as in a natural boundary layer.

In Fig. 21 measurements of the real part of the so-called narrow-band cross-correlation function for the u-component are presented. This function essentially indicates the degree of correlation at various frequencies between the longitudinal component fluctuations at pairs of points separated in the vertical direction. By making use of the von Kármán spectral model, it is possible to derive a theoretical relation for this function (Harris, 1970;

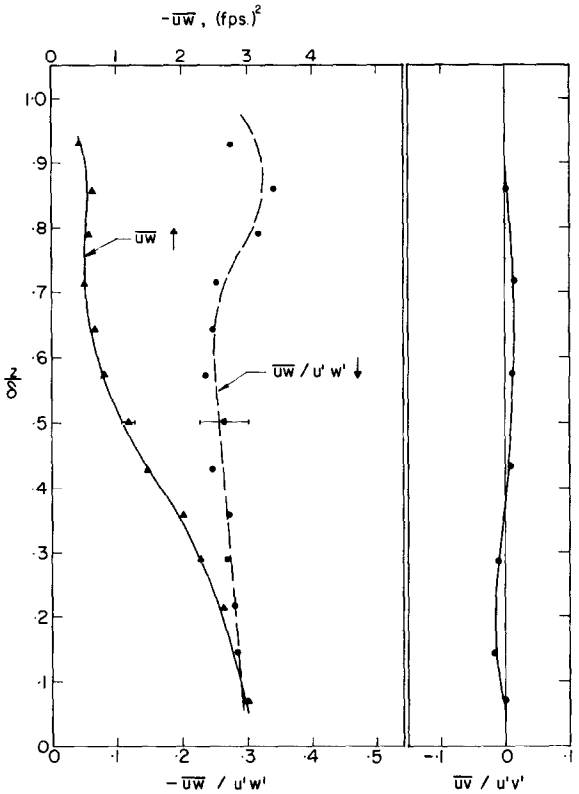

Fig. 20. Reynolds stress profiles at $x/H = 6.75$. Velocity profile $\alpha = 0.16$ set at $x/H = 6.75$ with roughness and 1 in. barrier.

Teunissen, 1970) which is also plotted in Fig. 21. In spite of a large amount of scatter in the experimental data, which is unavoidable due to the nature of the measurements, good agreement with the von Kármán model curve is observed. This degree of agreement is similar to that found by Harris (1970) at comparable heights in an atmospheric flow possessing a power-law mean velocity profile with $\alpha = 0.18$. In addition, further measurements at smaller heights in the present flow showed increasing departure of the experimental data from the theoretical curve, a result also observed by Harris in the planetary flow. This result is of course not unexpected since, strictly speaking, the von Kármán expression is valid only for isotropic turbulence and boundary layer flows tend in general to become more nearly isotropic with increasing height above the surface.

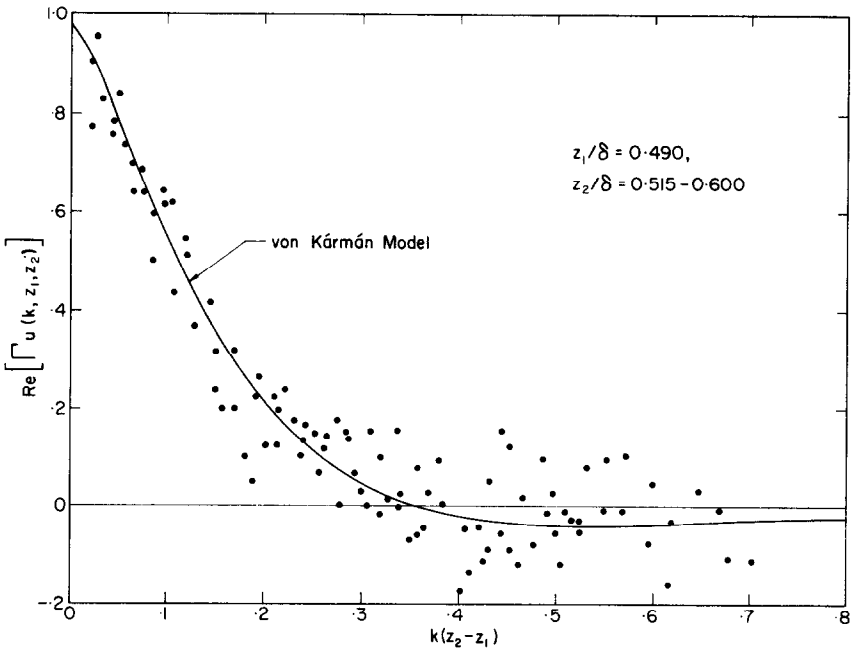

Fig. 21. Narrow-band cross-correlation function for points z_1 and z_2 at $x/H = 6.75$, $y/H = 0$. Velocity profile $\alpha = 0.16$ set at $x/H = 6.75$ with roughness and 1 in. barrier.

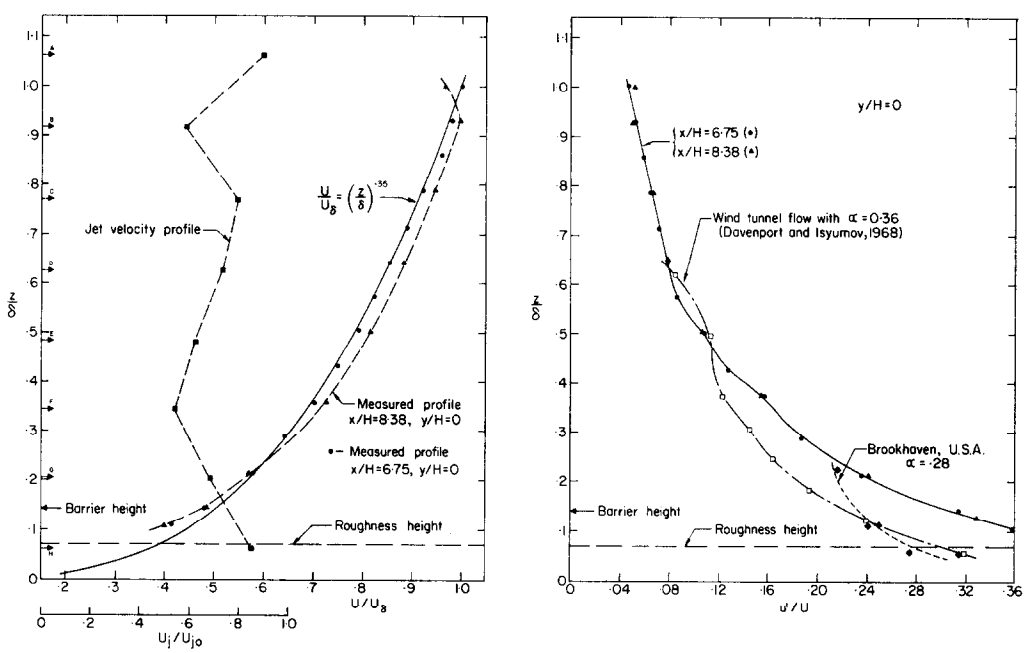

Fig. 22. Mean velocity and turbulence intensity profiles in flow set up to obtain $\alpha = 0.35$ velocity profile at $x/H = 6.75$ with roughness and 1 in. barrier.

4.6 *Simulated flow characteristics—*$\alpha = 0.35$

In order to produce a wind tunnel flow typical of the planetary flow over urban or built-up areas, the 1 in. barrier was placed at $x/H = 1.25$ and LEGO baseplate-plus-bricks was used to simulate the surface roughness. The jet velocities were then adjusted to produce a flow with a power-law mean velocity profile having $\alpha = 0.35$ at $x/H = 6.75$.

The mean velocity profile in the flow obtained is seen in Fig. 22 to have changed only slightly from $x/H = 6.75$ to $x/H = 8.38$. This change was likely due to excess roughness of the surface, although no change at all can be observed in the corresponding turbulence intensity profiles. Based on the comparison shown between the present data and those obtained in both boundary layer wind tunnel and planetary flows, it is felt that the intensity profile achieved here is quite good as a simulation of the corresponding atmospheric flow. In addition, the longitudinal component power spectrum obtained in this flow is seen in Fig. 23 to be in excellent agreement with both the shape and the location of the corresponding von Kármán model spectrum.

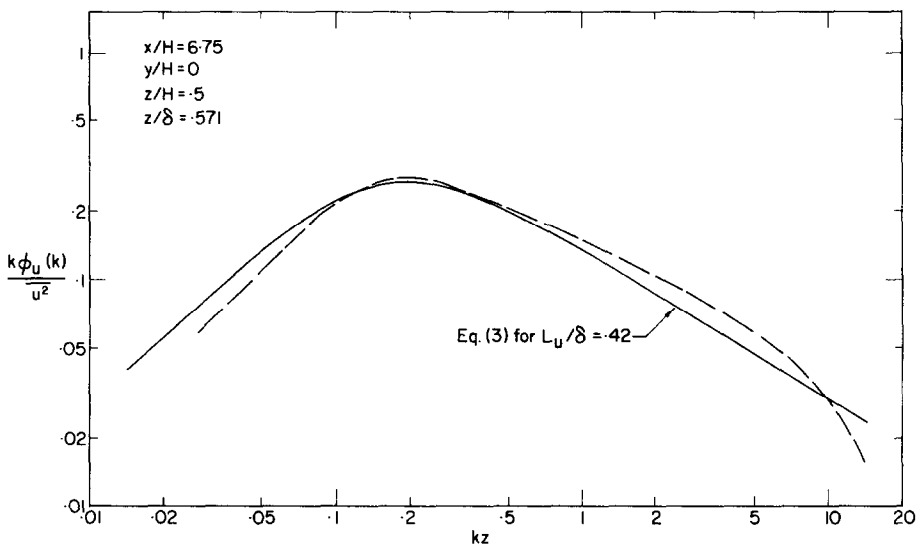

Fig. 23. Longitudinal component power spectrum for flow with $\alpha = 0.35$.

5. LINEAR SHEAR FLOWS

In addition to the planetary flow simulations described above, an investigation was carried out to determine the capability of the jet tunnel for producing two-dimensional, nearly homogeneous linear shear flows, i.e. flows in which the mean velocity has a constant, non-zero gradient in the vertical direction and a zero gradient in the lateral direction, and in which the turbulence properties are constant in a fixed cross-sectional plane of the flow and nearly constant in the longitudinal direction. Flows of this type are useful for determining the effect of various degrees of shear on structural and vehicle response, as well as for making fundamental studies of the nature of turbulent shear flows.

It was found in general that when the velocities of the jets in the grid were set to obey a linear mean velocity profile with a particular value of constant gradient, then the flow downstream of the jet mixing region possessed a linear mean velocity profile with a constant gradient which was roughly 0.37–0.44 times this value. In addition, little decay of

this profile was observed in the downstream direction. The magnitude of the gradient produced was somewhat larger than that which can be predicted using the simple ejector theory mentioned in Section 3.2, i.e. 0.27 times the input gradient. This difference must be attributed to the simplifying assumptions of the theory and jet interaction and wall effects, although the exact manner in which these effects might be handled is not at present clear.

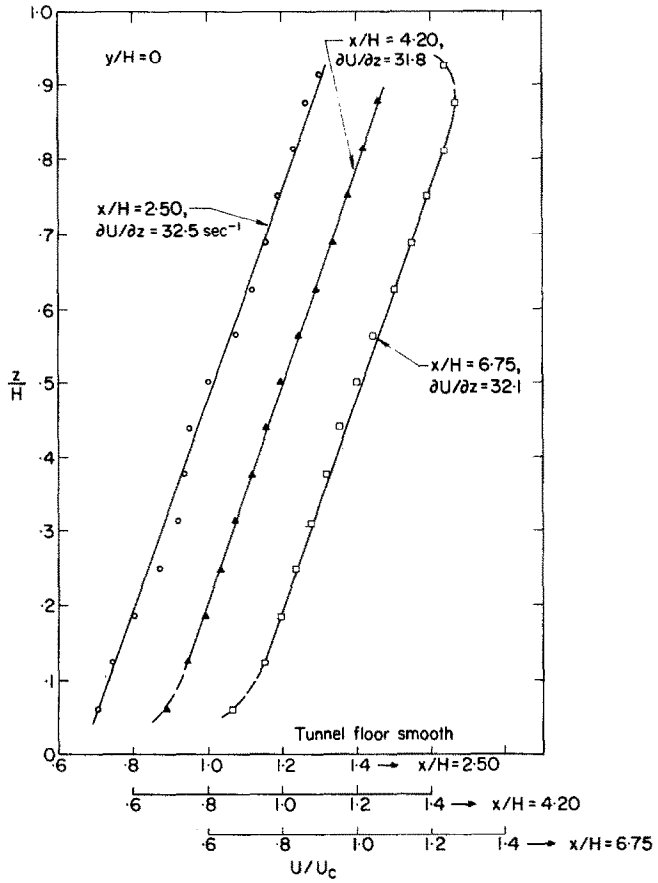

Fig. 24. Development of mean velocity profile in linear shear flow.

The results obtained are typified by the curves of Fig. 24. In this case the jets were set to follow a linear profile with a gradient of 86 s^{-1} and a gradient of about 32 s^{-1} was produced in the mixed-flow region of the tunnel. By appropriate adjustment of the jets, it was found possible to obtain virtually any desired value of constant mean velocity gradient in the mixed-flow region of the tunnel.

Typical results for the variation of turbulence characteristics across a fixed plane in a linear shear flow are given in Fig. 25. Within the accuracy of their measurement, the scales shown here are seen to be reasonably constant through the flow in spite of the mean velocity gradient of 31.8 s^{-1} in this plane. Also, tunnel centreline measurements indicated that a reasonable degree of homogeneity in the longitudinal direction was achieved beyond $x/H \sim 4$–5 in flows of this type. From these and other similar results, it was concluded

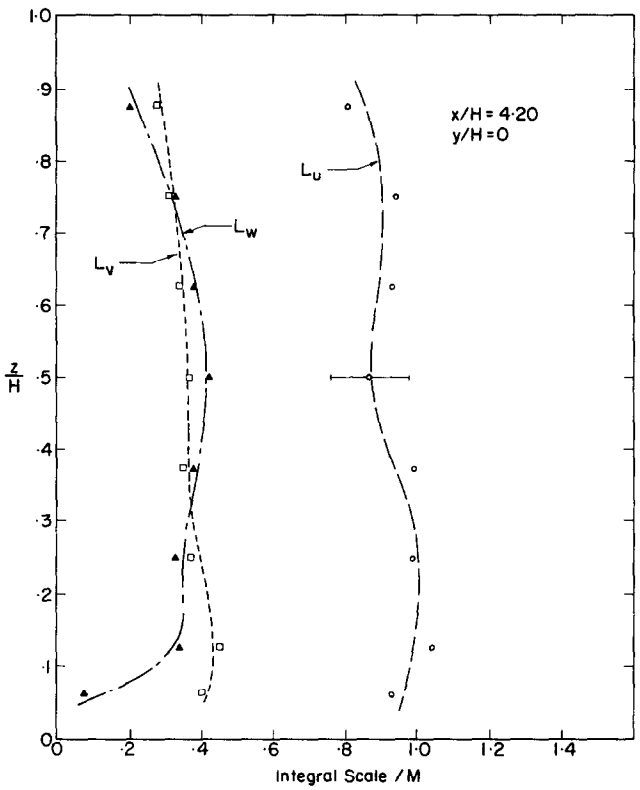

Fig. 25. Integral scale profiles in linear shear flow.

that the jet tunnel is indeed capable of producing nearly homogeneous linear shear flows with differing values of constant mean velocity gradient. Further details of the results obtained in these flows are given in Teunissen (1972).

6. RELATIVE MERITS OF THE JET TUNNEL

Planetary boundary layer simulation using the multiple-jet wind tunnel concept has both advantages and disadvantages when compared with other methods presently in use. Its primary advantage over a boundary layer tunnel lies in its length. For example, if it is assumed that about two tunnel heights are sufficient for the inlet and jet sections of such a tunnel, then a total length of about $10\,H$ should be sufficient, based on present results. More significantly, this corresponds to about 11–12 boundary layer heights, as compared with a value of about 20–25 δ required to develop a useful flow in a boundary layer tunnel. In addition, the relative ease with which particular velocity profiles may be produced by simple jet adjustment is an advantage in cases where departures from specific power-law profiles are required.

The chief disadvantage of the jet tunnel relative to a boundary layer tunnel is the power necessary to drive it. That is, the figures given in Section 3.1 may be used to approximately determine the power necessary to drive a jet tunnel of any particular dimensions. On this basis, it is estimated that the jet tunnel requires roughly three times the power used by a boundary layer tunnel to produce boundary layer flows of equal thickness.

As for comparison with the use of passive devices for boundary layer simulation, the jet tunnel has the advantage of being far more easily adjusted for producing desired flows as a result of the relative independence of the mean velocity and turbulence producing mechanisms. Further simplification could be achieved by the addition of a feedback system which would use the outputs of velocity sensors in or near the tunnel test section to control the velocity settings of the jets. This would permit "automatic" setting and maintenance of desired velocity profiles instead of the iterative procedure presently used. A significant disadvantage of the jet approach is of course the fact that it is not as readily adaptable to existing wind tunnels as are most of the other devices now being used.

Another potential advantage of the jet tunnel that has not been explored in the present investigation is an ability to produce thermally stratified flows quite easily. The jet tunnel would appear to be ideally suited for this purpose since one could simply supply all the jets in a particular row of the grid from a single plenum chamber. This plenum could then be heated to the temperature required to produce a particular temperature profile in the mixed flow region of the tunnel.

Finally, the capability of the jet tunnel for producing turbulent flows other than planetary boundary layer simulations is a definite advantage insofar as its usefulness as a basic research tool is concerned. Consequently, as one would of course expect, the relative merits of the jet tunnel as a laboratory facility are fundamentally dependent on the uses for which it is intended.

7. SUMMARY OF CONCLUSIONS

The main conclusions arrived at as a result of the present investigation are summarized as follows:

(1) The jet tunnel is capable of producing, by appropriate adjustment of the jets, turbulent flows possessing virtually any desired mean velocity profile at any location beyond about two tunnel heights from the jets.

(2) Turbulence intensities in a given flow may be altered with the use of devices such as simple "tripping" barriers, while desired mean velocity profiles can simultaneously be retained by appropriate jet velocity adjustment.

(3) The jet tunnel provides an excellent method for simulating the flows found in the planetary boundary layer with respect to the mean velocity and turbulence characteristics. A total tunnel length of roughly 11–12 boundary layer heights should be sufficient for this purpose.

(4) The jet tunnel is capable of producing nearly homogeneous two-dimensional linear shear flows with differing values of constant mean velocity gradient. Reasonable longitudinal homogeneity is obtained beyond about 4–5 tunnel heights downstream of the jet grid.

8. FUTURE WORK

As a result of the success of the present investigation, the original UTIAS subsonic wind tunnel has been modified into the multiple-jet configuration (Teunissen and Schuyler, 1974). Planned work in this facility includes structural response studies and the measurement of correlations of the turbulence encountered by STOL aircraft along typical landing paths through a neutrally stable boundary layer.

Future work into the jet tunnel concept itself should likely take the form of an investigation into its capability for producing thermally stratified flows. In addition, further investigation into the effects of barriers and perhaps other devices on the flows produced could

be undertaken. Possible alterations to the tunnel roof that might alleviate the problem of small values of L_w in the upper regions of the planetary boundary layer simulations should also be investigated.

Acknowledgements—The author would like to express his deep appreciation to Professor Bernard Etkin for his guidance and encouragement throughout the performance of this work. Financial support was received from the National Research Council of Canada and from the United States Air Force under RTD Contract No. F-33(615)-68-C1005.

REFERENCES

Baines W. D. (1965) Effects of velocity distribution on wind loads and flow patterns on buildings. Paper 6, *Int. Conf. on Wind Effects on Buildings and Structures*, held at N.P.L., H.M.S.O., London.

Baines W. D. and Peterson E. G. (1951) An investigation of the flow through screens. *Trans. A.S.M.E.*

Batchelor G. K. and Townsend A. A. (1948) Decay of isotropic turbulence in the initial period. *Proc. R. Soc. London*, Ser. **A,** 1035.

Cermak J. E. (1970) Laboratory simulation of the atmospheric boundary layer. *A.I.A.A.* Paper 70–751.

Counihan J. (1969) An improved method of simulating an atmospheric boundary layer in a wind tunnel. *Atmospheric Environment* **3,** 197–214.

Counihan J. (1970) Further measurements in a simulated atmospheric boundary layer. *Atmospheric Environment* **4,** 259–275.

Davenport A. G. (1965) The relationship of wind structure to wind loading. Paper 2, *Int. Conf. on Wind Effects on Buildings and Structures*, held at N.P.L., H.M.S.O., London.

Davenport A. G. and Isyumov N. (1968) The application of the boundary layer wind tunnel to the prediction of wind loading. *Proc. Int. Research Seminar on Wind Effects on Buildings and Structures*, held at N.R.C., University of Toronto Press, Canada.

Harris R. I. (1968) Measurements of wind structure at heights up to 598 ft above ground level. E.R.A. Technical Report 5258 (unpublished).

Harris R. I. (1970) The nature of the wind. Presented at the *Construction Industry Research and Information Association Seminar on the Modern Design of Wind-Sensitive Structures*, held in London, England.

Klebanoff P. S. (1956) Characteristics of turbulence in a boundary layer with zero pressure gradient. NACA Report 1247.

Lau Y. L. (1966) The flow of stratified and homogeneous fluids through curved screens. U.T. Mech. E TP 6604, University of Toronto, Canada.

Ludwig G. R. and Sundaram T. R. (1969) On the laboratory simulation of small-scale atmospheric motions. Cornell Aero. Lab. Report No. VC-2740-S-1, Cornell University, U.S.A.

Schon J. P. and Mery P. (1971) A preliminary study of the simulation of neutral atmospheric boundary layer in a wind tunnel. *Atmospheric Environment* **5,** 299–311.

Standen N. M. (1972) A spire array for generating thick turbulent shear layers for natural wind simulation in wind tunnels. NAE Report LTR-LA-94, N.R.C., Canada.

Strom G. H. and Kaplan E. J. (1960) Convective turbulence of wind tunnel project. U.S. A.E.C. ANL 6199, Argonne, Ill., U.S.A.

Sundaram T. R., Skinner G. T. and Ludwig G. R. (1970) Simulation of small-scale atmospheric phenomena. Cornell Aero. Lab. Report No. VC-2697-A-1, Cornell University, U.S.A.

Surry D. (1969) The effect of high intensity turbulence on the aero-dynamics of a rigid circular cylinder at subcritical Reynolds number. UTIAS Report No. 142, University of Toronto, Canada.

Templin R. J. (1969) Interim progress note on simulation of earth's surface winds by artificially thickened wind tunnel boundary layers. NAE Report LTR-LA-22, N.R.C., Canada.

Teunissen H. W. (1969) An ejector-driven wind tunnel for the generation of turbulent flows with arbitrary mean velocity profile. UTIAS Tech. Note No. 133, University of Toronto, Canada.

Teunissen H. W. (1970) Characteristics of the mean wind and turbulence in the planetary boundary layer. UTIAS Review No. 32, University of Toronto, Canada.

Teunissen H. W. (1972) Simulation of the planetary boundary layer in a multiple-jet wind tunnel. UTIAS Report No. 182, University of Toronto, Canada.

Teunissen H. W. and Schuyler G. (1974) Design and calibration of the UTIAS boundary layer simulation wind tunnel. UTIAS Tech. Note No. 186, University of Toronto, Canada (to be published).

Vickery B. J. (1965) On the flow behind a coarse grid and its use as a model of atmospheric turbulence in studies related to wind loads on buildings. N.P.L. Aero Report 1143, London.